S1. Calibrations

We homogenized the SST assessments across the study area by applying the MgCaRB calibration (Gray et al., 2018) for Mg/Ca and the BAYSPLINE calibration (J. E. Tierney & Tingley, 2018) for $U_{37}^{K'}$ (Jonkers et al., accepted). In rare cases, where raw data were not available, it was necessary to back-calculate Mg/Ca or $U_{37}^{K'}$ from published SST data before applying the global calibrations.

While the results of $U_{37}^{K'}$-SSTs from the application of the original and homogenized calibration equations are mostly within error (Fig. S1), Mg/Ca-derived SSTs (original vs. homogenized) partly show large deviations (Fig. S1). These likely result from the consideration of potential salinity and alkalinity changes in homogenized SSTs from the different core sites, which are not considered in (most) original calibrations. Of all records, 36 Mg/Ca and 24 $U_{37}^{K'}$ records extend into the Common Era (CE). For these records, we calculated mean CE SSTs and compared the results to the COBE SSTs (Fig. S2). We find that SSTs calculated with the original calibrations show smaller offsets (calculated as mean absolute deviations from the COBE SSTs) than the homogenized SSTs (Tables S.2 and S3). Furthermore, the application of the MgCaRB calibration also leads to a larger site to site variability of SST estimates and an enhanced mismatch between $U_{37}^{K'}$ and Mg/Ca-derived SSTs (Fig. S3). We therefore base our analysis of proxy-derived SST anomalies on the SST assessments that result from the application of the calibration equations used in the original publications of the records.

S2. Age models

The age models of the records included in the PalMod data synthesis v2 (Jonkers et al., accepted) base on a combination of absolute age control points from tephra layers, from radiocarbon dates, and the alignment of benthic foraminifera $\delta^{18}O$ records to regional benthic $\delta^{18}O$ stacks (Lisiecki & Stern, 2016). All radiocarbon ages were converted to calendar ages using the IntCal20 calibration curve (Reimer et al., 2020). To account for the variability of marine reservoir ages in space and time, the reservoir age estimates of the comprehensive ocean general circulation model of Butzin et al. (2017) were applied. To avoid inflating confidence in the tuned age models and to ensure comparability between different cores, tie points were preferentially set at the position of marine isotope stage boundaries. Uncertainty estimates of the tie points are based on the chronological uncertainty of the $\delta^{18}O$ stacks, as reported by Lisiecki and Stern (2016).

S3. Model simulations

The atmosphere is represented by the Community Atmosphere Model (CAM5) with a horizontal resolution of 1.9 x 2.5° and 30 vertical levels, while the ocean model (POP2) has a nominal resolution of 1° with 60 depth levels. The ocean grid is refined meridionally near the equator (~0.26°) to improve simulation accuracy in this dynamically active region. CESM further includes the Community Land Model (CLM4), which uses a nominal 2° grid in our simulations. CLM4 does not include a fully dynamic vegetation, such that the spatial distributions of plant functional types (PFT) are prescribed. However, CLM4 runs with a prognostic phenology provided by its

carbon-nitrogen cycle model, such that the simulation of leaf and stem area indices as well as vegetation height is interactive.

Table S1. Summary of SST records used in this study.

Site	Longitude	Latitude	Water depth	Proxy	Reference dois[1]	References[1]
130-806B	159.36	0.32	2519.9	Mg/Ca	10.1126/science.1115933	Medina-Elizalde and Lea (2005)
167-1014	-119.98	32.83	1165.8	UK´37	10.1029/2004GL020138	Yamamoto et al. (2004)
167-1019C	-124.93	41.68	946.9	UK´37	10.1029/2002PA000768	Barron et al. (2003)
184-1143	113.29	9.36	2772.3	UK´37	10.1016/j.epsl.2011.04.016	Li et al. (2011)
184-1146	116.27	19.46	2091.5	UK´37	10.1126/science.1185435	Herbert et al. (2010)
202-1240	-86.46	0.02	2920.8	Mg/Ca	10.1029/2008PA001620	Pena et al. (2008)
202-1242	-83.61	7.86	1363.7	Mg/Ca	10.1029/2005PA001208	Benway et al. (2006)
3cBx	139.64	8.02	2829	Mg/Ca	10.1016/j.palaeo.2012.06.002	Sagawa et al. (2012)
A7	127.02	28.01	1264	Mg/Ca	10.1029/2004PA001061	Sun et al. (2005)
AAS-9-21	72.65	14.51	1807	Mg/Ca	10.1029/2008PA001687	Govil and Naidu (2010)
BJ8-03-13GGC	115.2	7.45	2924	Mg/Ca	10.1038/NGEO920	Linsley et al. (2010)
BJ8-03-70GGC	119.39	3.55	482	Mg/Ca	10.1038/NGEO920	Linsley et al. (2010)
GeoB10029-4	100.13	-1.49	964	Mg/Ca	10.1016/j.epsl.2010.01.024	M. Mohtadi, Steinke, et al. (2010)
GeoB10038-4	103.25	-5.94	1819	UK´37	10.1016/j.epsl.2010.01.024, 10.1016/j.quascirev.2009.12.006	M. Mohtadi, Lückge, et al. (2010); M. Mohtadi, Steinke, et al. (2010)
GeoB10042-1	104.64	-7.11	2460	Mg/Ca	10.1002/2015PA002802	Setiawan et al. (2015)
GeoB10043-3	105.06	-7.31	2172	Mg/Ca	10.1002/2015PA002802	Setiawan et al. (2015)
GeoB10069-3	120.92	-9.59	1250	Mg/Ca	10.1016/j.epsl.2013.11.032	Gibbons et al. (2014)
GeoB12605-3	39.11	-5.57	195	Mg/Ca	10.1002/2013PA002555	Kuhnert et al. (2014)
GeoB12610-2	39.42	-4.82	399	Mg/Ca	10.1002/jqs.2767	Rippert et al. (2015)
GeoB12615-4	39.84	-7.14	446	Mg/Ca	10.5194/cp-10-293-2014	Romahn et al. (2014)
GeoB16602	113.71	18.95		UK´37	10.1016/j.epsl.2018.04.046 10.1038/s41561-018-0250-1	E. Huang et al. (2018) Cheng et al. (2018)
GeoB17426-3	150.86	-2.19	1367	Mg/Ca	10.1029/2019PA003832	Hollstein et al. (2020)
GeoB5844-2	34.68	27.71	963	UK´37	10.1029/2002PA000864	Arz et al. (2003)
GeoB7186-3	-75.16	-44.15	1169	UK´37	10.1016/j.quascirev.2006.12.008	Mahyar Mohtadi et al. (2007)
GIK17286-1	89.88	19.74	1428	UK´37	10.1029/2019PA003646	Lauterbach et al. (2020)
GIK17748-2	-72.03	-32.75	2545	UK´37	10.1016/S0277-3791(02)00012-4	J.-H. Kim et al. (2002)
GIK17927-2	119.45	17.25	2804	UK´37	10.1007/s00531-015-1227-6	Sadatzki et al. (2016)
GIK17940-2	117.38	20.12	1727	UK´37	10.1029/1998PA900015	Pelejero et al. (1999)
GIK17954-2	111.53	14.8	1520	UK´37	10.1029/1998PA900015	Pelejero et al. (1999)
GIK17961-2	112.33	8.51	1795	UK´37	10.1029/1998PA900015; 10.1016/S0025-3227(98)00182-0	Pelejero et al. (1999); L. Wang et al. (1999)
GIK18287-3	110.66	5.66	598	UK´37	10.1006/qres.2001.2235	Steinke et al. (2001)
GIK18471-1	129.98	-9.37	485	Mg/Ca	10.1016/j.palaeo.2016.09.010	Cappelli et al. (2016)
GiK18515-3	119.36	-3.63	688	Mg/Ca	10.1016/j.quascirev.2016.10.018	Schröder et al. (2016)
GIK18519-2	118.11	-0.57	1658	Mg/Ca	10.1029/2018PA003323	Schröder et al. (2018)
GIK18522-3	119.08	1.4	975	Mg/Ca	10.1029/2018PA003323	Schröder et al. (2018)
GIK18526-3	118.17	-3.61	1524	Mg/Ca	10.1029/2018PA003323	Schröder et al. (2018)
GIK18540-3	119.58	-6.87	1189	Mg/Ca	10.1029/2018PA003323	Schröder et al. (2018)
KNR195-5-CDH23	-81.13	-3.75	373	UK´37	10.1002/2015PA002816	Bova et al. (2015)
KNR195-5-CDH26	-81.31	-3.99	1023	UK´37	10.1002/2015PA002816	Bova et al. (2015)
KT05-7-PC-02	140.77	41	61	UK´37	10.1016/j.quascirev.2008.12.009	Kawahata et al. (2009)
KX973-21-2	157.98	-1.42	1897	Mg/Ca	10.1126/sciadv.abc0402; 10.1038/s41586-022-05302-y	Dang et al. (2020); Jian et al. (2022)
KX973-22-4	159.25	-0.03	2362	Mg/Ca	10.1007/s00343-017-6082-9; 10.1038/s43247-021-00305-5	Zhang et al. (2017); Zhang et al. (2021)
LPAZ21P	-109.47	22.98	624	UK´37	10.1126/science.1059209	Herbert et al. (2001)
M75-3-137-3	37.87	-18.24	1339	UK´37	10.1002/palo.20053	Y. V. Wang et al. (2013)
M77-2-056-5	-81.12	-3.75	355	Mg/Ca	10.1002/2014PA002706	Nürnberg et al. (2015)
M77-2-059-1	-81.32	-3.95	997	UK´37	10.1002/2014PA002706	Nürnberg et al. (2015)
MD01-2378	121.79	-13.08	1783	Mg/Ca	10.1029/2006PA001278; 10.1016/j.epsl.2008.06.029; 10.1029/2008PA001653	Xu et al. (2006); Xu et al. (2008); Zuraida et al. (2009); (Holbourn et al., 2005)
MD01-2386	129.79	1.13	2816	Mg/Ca	10.1073/pnas.1915510117	Jian et al. (2020)
MD01-2390	113.41	6.64	1545	Mg/Ca	10.1016/j.quascirev.2007.12.003	Steinke et al. (2008)
MD01-2412	145	44.53	1225	UK´37	10.1016/j.gloplacha.2006.01.010	Harada et al. (2006)
MD01-2421	141.78	36.02	2224	UK´37	10.1029/2004GL021903	Yamamoto et al. (2005)
MD02-2529	-84.12	8.21	1619	UK´37	10.1038/nature05578	Leduc et al. (2007)
MD03-2607	137.41	-36.96	865	UK´37	10.1002/palo.20035	Lopes dos Santos et al. (2013)
MD03-2611G	136.55	-36.73	2420	UK´37	10.1016/j.quascirev.2020.106593	De Deckker et al. (2020)
MD05-2896	111.44	8.82	1657	UK´37	10.1016/j.yqres.2014.12.003	Dong et al. (2015)
MD05-2897	111.43	8.83	1658	UK´37	10.1016/j.yqres.2014.12.003	Dong et al. (2015)
MD05-2904	116.25	19.46	2066	Mg/Ca	10.1016/j.gloplacha.2011.06.006	Steinke et al. (2011)
MD05-2920	144.53	-2.86	1843	Mg/Ca	10.1016/j.quascirev.2013.12.018	Tachikawa et al. (2014)
MD05-2925	151.46	-9.34	1661	Mg/Ca	10.5194/cp-10-2253-2014; 10.1038/s41598-017-04031-x; 10.1016/j.quascirev.2022.107756	Lo et al. (2014); Lo et al. (2017); Lo et al. (2022)
MD06-3018	166.15	-23	2470	Mg/Ca	10.1029/2010PA002019	Russon et al. (2011)

MD06-3047B	124.8	17.01	2510	Mg/Ca	10.1016/j.palaeo.2017.12.039	Jia et al. (2018)
MD06-3067	126.5	6.51	1575	Mg/Ca	10.1029/2010PA001966	Bolliet et al. (2011)
MD06-3075	125.83	6.48	1878	UK´37	10.1002/2013PA002599	Fraser et al. (2014)
MD10-3340	128.72	-0.52	1094	Mg/Ca	10.1126/sciadv.abc0402, 10.1038/s41586-022-05302-y	Dang et al. (2020); Jian et al. (2022)
MD161-17	82.02	16.06	790	Mg/Ca	10.1002/2017GC007075	Panmei et al. (2017)
MD77-194	75.23	10.47	1222	UK´37	10.1016/S0277-3791(97)00099-1	Sonzogni et al. (1998)
MD79-257	36.2	-20.24	1262	UK´37	10.1016/S0277-3791(97)00099-1	Sonzogni et al. (1998)
MD90-963	73.53	5.04	2446	UK´37	10.1016/S0967-0645(97)00008-8	Rostek et al. (1997)
MD96-2048	34.02	-26.17	660	UK´37	10.5194/cp-7-1285-2011	Caley et al. (2011)
MD97-2121	177.99	-40.38	3014	UK´37	10.1029/2005PA001191	Pahnke and Sachs (2006)
MD97-2125	161.44	-22.34	1684	UK´37	10.1016/j.quascirev.2008.12.013	Tachikawa et al. (2009)
MD97-2138	146.23	-1.25	1900	UK´37	10.1029/2006PA001269	de Garidel-Thoron et al. (2007)
MD97-2140	141.76	2.04	2547	Mg/Ca	10.1038/nature03189	de Garidel-Thoron et al. (2005)
MD97-2141	141.29	8.79	3633	Mg/Ca	10.1029/2001GC000260; 10.1029/2000PA000557; 10.1029/2021PA004361	Oppo et al. (2003); de Garidel-Thoron et al. (2001); Weiss et al. (2022)
MD97-2142	119.47	12.69	1557	UK´37	10.3319/TAO.2008.19.4.363(IMAGES)	Shiau et al. (2008)
MD97-2151	109.87	8.73	1598	UK´37	10.1016/j.palaeo.2005.11.033	Zhao et al. (2006)
MD98-2152	103.88	-6.33	1796	UK´37	10.1016/j.epsl.2019.03.038	Windler et al. (2019)
MD98-2160	117.49	-5.20	1185	Mg/Ca	10.1029/2006GL027234	Newton et al. (2006)
MD98-2161	117.49	-5.22	1185	Mg/Ca	10.1016/j.gloplacha.2013.08.017; 10.1038/s41598-018-24055-1	Fan et al. (2013); Fan et al. (2018)
MD98-2162	117.9	-4.69	1855	Mg/Ca	10.1038/s41586-022-05302-y	Jian et al. (2022)
MD98-2165	118.33	-9.65	2100	Mg/Ca	10.1029/2006GC001514	Levi et al. (2007)
MD98-2170	125.39	-10.59	832	Mg/Ca	10.1126/science.1143791	Stott et al. (2007)
MD98-2176	133.44	-5	2382	Mg/Ca	10.1038/nature02903	Stott et al. (2004)
MD98-2178	118.7	3.62	1984	Mg/Ca	10.1016/j.gloplacha.2013.08.017; 10.1038/s41598-018-24055-1	Fan et al. (2013); Fan et al. (2018)
MD98-2181	125.83	6.3	2114	Mg/Ca	10.1016/j.quascirev.2009.05.007; 10.1126/science.1071627	Saikku et al. (2009); Stott et al. (2002)
MD98-2188	123.49	14.82	730	Mg/Ca	10.1029/2011GL050154	Dang et al. (2012)
ME0005A-24JC	-86.46	0.02	2941	UK´37	10.1038/nature05222; 10.1016/j.quascirev.2010.10.012	Kienast et al. (2006); Dubois et al. (2011)
ME0005A-27JC	-82.79	-1.85	2203	UK´37	10.1016/j.quascirev.2010.10.012	Dubois and Kienast (2011)
ME0005A-43JC	-83.61	7.86	1368	Mg/Ca	10.1029/2005PA001208	Benway et al. (2006)
ODP1012	-118.38	32.28	1783	UK´37	10.1126/science.1059209	Herbert et al. (2001)
ODP1016C	-122.28	34.53	3834	UK´37	10.1016/j.quascirev.2006.07.014	Yamamoto et al. (2007)
ODP1020	-126.43	41	3042	UK´37	10.2973/odp.proc.sr.167.206.2000; 10.1029/98pa00069	Heusser et al. (2000); Herbert et al. (1998)
ODP1239	-82.08	-0.67	1414	UK´37	10.1029/2009PA001868; 10.1002/2015PA002873; 10.1016/j.epsl.2010.06.010	Rincón-Martínez et al. (2010); Dyez et al. (2016); Etourneau et al. (2010)
ODP807	156.62	3.61	2804	Mg/Ca	10.1038/s41586-022-05302-y	Jian et al. (2022)
ODP846	-90.82	-3.1	3296	UK´37	10.1126/science.1120395	Lawrence et al. (2006)
P178-15P	44.3	11.96	869	UK´37, Mg/Ca	10.1038/NGEO2603	Jessica E. Tierney et al. (2016)
SCS90-36	111.49	18	2050	UK´37	10.1016/S0377-8398(97)00014-5	C.-Y. Huang et al. (1997)
SK157-4	78	2.67	3500	Mg/Ca	10.1029/2005GL024093	Saraswat et al. (2005)
SK17	72.97	15.25	840	Mg/Ca	10.1029/2007PA001564	Anand et al. (2008)
SK218-1	82	14.04	3307	Mg/Ca	10.1002/jqs.1392; 10.1016/j.quascirev.2011.10.004	Naidu and Govil (2010); Govil and Naidu (2011)
SK237-GC04	75	10.98	1245	Mg/Ca	10.1016/j.epsl.2013.05.022	Saraswat et al. (2013)
SO139-74KL	103.83	-6.54	1690	UK´37, Mg/Ca	10.1029/2008PA001627; 10.1016/j.quascirev.2018.05.035	Lückge et al. (2009) X. Wang et al. (2018)
SO18480	121.65	-12.06	2299	Mg/Ca	10.1126/sciadv.abc0402; 10.1038/s41586-022-05302-y	Dang et al. (2020); Jian et al. (2022)
SO189-119KL	96.31	3.52	808	Mg/Ca	10.1038/nature13196	M. Mohtadi et al. (2014)
SO189-39KL	99.91	-0.79	517	Mg/Ca	10.1038/nature13196	M. Mohtadi et al. (2014)
SO217-18517-2	117.56	-1.54	698	UK´37, Mg/Ca	10.1002/2016PA003030	Hendrizan et al. (2017)
SO42-74KL	57.35	14.32	3212	UK´37	10.1016/j.quascirev.2004.08.010	Jung-Hyun Kim et al. (2004)
TR163-19	-90.95	2.26	2348	UK´37, Mg/Ca	10.1029/2009PA001781; 10.1126/science.289.5485.1719	Dubois et al. (2009); D. W. Lea et al. (2000)
TR163-22	-92.4	0.52	2830	Mg/Ca	10.1016/j.quascirev.2005.11.010	David W. Lea et al. (2006)
U1429	129	31.62	732	UK´37	10.1038/s41467-018-05814-0	Clemens et al. (2018)
U1446	85.73	19.08	1440	Mg/Ca	10.1126/sciadv.abg3848; 10.1038/s43247-021-00133-7	Clemens et al. (2021); Nilsson-Kerr et al. (2021)
U1448	93	10.63	1097	Mg/Ca	10.1016/j.quascirev.2022.107403; 10.1038/s43247-021-00133-7	Nilsson-Kerr et al. (2022); Nilsson-Kerr et al. (2021)
V19-27	-82.07	-0.47	1373	UK´37	10.1029/2008PA001593	Koutavas and Sachs (2008)
V19-28	-84.65	-2.37	2720	UK´37	10.1029/2008PA001593	Koutavas and Sachs (2008)
V19-30	-83.52	-3.38	3091	UK´37	10.1029/2008PA001593	Koutavas and Sachs (2008)
W8402A-14	-138.96	0.95	4287	UK´37	10.1029/94PA02116	Jasper et al. (1994)
WIND-28K	51.01	-10.15	4157	Mg/Ca	10.1002/2013GC004994; 10.1029/2006GL027097	Johnstone et al. (2014); Kiefer et al. (2006)

[1]includes references of SST records, radiocarbon dates of the records, and isotope records used to generate the age models.

Table S2. Comparison of proxy-based SSTs of the Common Era resulting from (i) the application of the original calibration and (ii) the MgCaRB calibration and COBE SST data. For each record, the calibration that results in SST closer to COBE SST is typed in bold.

Site	COBE SST (°C)	Original SST (°C)	MgCaRB SST (°C)	Original SST – COBE SST (°C)	MgCaRB SST – COBE SST (°C)
202-1240	24.6	24.7	19.0	**0.1**	-5.5
202-1242	28.0	26.9	26.5	**-1.1**	-1.6
A7	23.8	26.7	26.9	**2.9**	3.1
AAS-9-21	27.8	28.8	28.5	1.0	**0.7**
BJ8-03-13GGC	28.3	27.4	28.6	-0.9	**0.3**
GeoB10038-4	28.3	25.0	26.3	-3.3	**-2.0**
GeoB10043-3	28.0	26.9	26.5	**-1.1**	-1.6
GeoB10069-3	28.0	27.2	26.0	**-0.8**	-2.0
GeoB12605-3	26.9	26.7	28.2	**-0.2**	1.3
GeoB12610-2	26.9	27.8	26.6	1.0	**-0.2**
GeoB12615-4	27.0	28.6	28.0	1.6	**1.0**
GIK18519-2	28.8	27.8	29.3	-1.0	**0.5**
GIK18526-3	28.7	28.0	29.5	**-0.7**	0.8
M75-3-137-3	26.3	24.4	24.9	-1.9	**-1.4**
MD01-2378	28.3	27.9	28.9	**-0.4**	0.6
MD01-2390	28.2	27.6	27.4	**-0.6**	-0.8
MD05-2904	26.3	26.4	24.8	**0.1**	-1.5
MD05-2925	28.1	27.8	28.7	**-0.2**	0.7
MD10-3340	28.4	28.9	28.9	0.5	**0.5**
MD98-2160	28.6	28.9	30.8	**0.4**	2.3
MD98-2161	28.6	27.7	29.1	-0.8	**0.5**
MD98-2162	28.5	28.4	28.1	**-0.1**	-0.4
MD98-2165	27.9	27.6	26.8	**-0.2**	-1.1
MD98-2176	27.8	28.9	30.2	**1.0**	2.4
MD98-2178	28.5	27.5	28.7	-1.0	**0.2**
MD98-2181	28.3	29.2	30.7	**0.9**	2.4
MD98-2188	28.0	28.7	29.8	**0.6**	1.7
P178-15P	28.1	27.7	28.0	-0.3	**0.0**
SK17	27.7	26.5	27.8	-1.3	**0.1**
SK218-1	28.1	29.0	29.9	**0.9**	1.9
SK237-GC04	27.9	28.4	28.9	**0.5**	1.0
SO18480	28.3	28.2	28.0	**-0.1**	-0.3
SO189-119KL	28.8	29.6	30.6	**0.9**	1.8
SO189-39KL	28.6	29.7	30.2	**1.1**	1.7
TR163-22	24.0	24.4	18.5	**0.3**	-5.5
U1446	27.7	28.5	29.8	**0.8**	2.1
			Average absolute deviation:	**0.9**	**1.4**

Table S3. Same as Table S2, but for $U_{37}^{K'}$ – SSTs applying (i) the original calibrations and (ii) the BAYSPLINE calibration.

Site	COBE SST (°C)	Original SST (°C)	BAYSPLINE SST (°C)	Original SST – COBE SST (°C)	BAYSPLINE SST – COBE SST (°C)
167-1019C	11.0	11.4	11.0	0.5	**0.0**
GeoB10038-4	28.3	27.7	28.9	-0.6	**0.6**
GeoB5844-2	24.7	26.7	28.0	**2.0**	3.3
GeoB7186-3		13.6	13.1		
GIK17286-1	27.6	28.5	29.2	**0.9**	1.6
GIK17940-2	25.9	26.8	27.2	**0.9**	1.3
GIK17954-2	27.1	27.0	27.4	**-0.2**	0.3
KNR195-5-CDH23	21.8	23.3	22.7	1.6	**0.9**
KT05-7-PC-02	12.1	23.1	22.4	11.0	**10.3**
LPAZ21P	24.3	25.1	25.6	**0.8**	1.3
M75-3-137-3	26.3	27.6	28.3	**1.3**	2.0
M77-2-059-1	21.8	21.9	21.1	**0.1**	-0.7
MD01-2412	6.0	12.4	11.9	6.4	**5.9**
MD02-2529	27.9	28.9	28.5	1.0	**0.6**
MD03-2607	16.1	18.3	17.6	2.2	**1.5**
MD03-2611G	16.0	18.7	17.9	2.7	**1.9**
MD06-3075	28.3	28.4	29.1	**0.1**	0.8
MD77-194	27.9	27.5	29.3	**-0.4**	1.4
MD79-257	26.0	26.9	27.9	**0.9**	1.9
MD97-2151	27.7	27.4	27.8	-0.3	**0.2**
P178-15P	28.1	28.4	29.2	**0.4**	1.2
SO42-74KL	26.2	27.2	28.9	**1.0**	2.7
U1429	21.9	23.8	23.9	1.9	**1.9**
V19-27	24.3	26.2	27.3	**1.8**	3.0
167-1019C	11.0	11.4	11.0		
			Average absolute deviation:	**1.6**	**1.9**

Table S4. Summary of calculated mean SST anomalies (°C) for the South China Sea (SCS), Western Pacific Warm Pool (WPWP) and eastern equatorial Pacific (EEP) areas

	SCS (108°E, 21°N - 120°E, 5°N)			**WPWP (138°E, 10°N - 160°E, 10°S)**			**EEP (93°W, 10°N - 80°W. 5°S)**		
	Proxy-based	**without expanded vegetation**	**with expanded vegetation**	**Proxy-based**	**without expanded vegetation**	**with expanded vegetation**	**Proxy-based**	**without expanded vegetation**	**with expanded vegetation**
6 ka	0.1	-0.5	0.0	0.1	-0.3	0.1	-0.1	-0.4	-0.2
127 ka	0.4	-0.8	-0.3	0.8	-0.3	0.4	1.9	-0.2	0.2
409 ka	0.3	-0.5	0.0	0.5	0.0	0.5	2.0	-0.2	0.1

Fig. S1. Comparison of SSTs resulting from the application of the original and homogenized proxy-SST calibrations. Mean mid-Holocene SSTs of all records resulting from the application of original and homogenized (updated) proxy-SST calibrations. Black and red dots indicate SST estimates based on Mg/Ca and UK'37. Whiskers show the 16.6th and 83.3rd (thick line) 2.5th and 97.5th (thin line) percentiles.

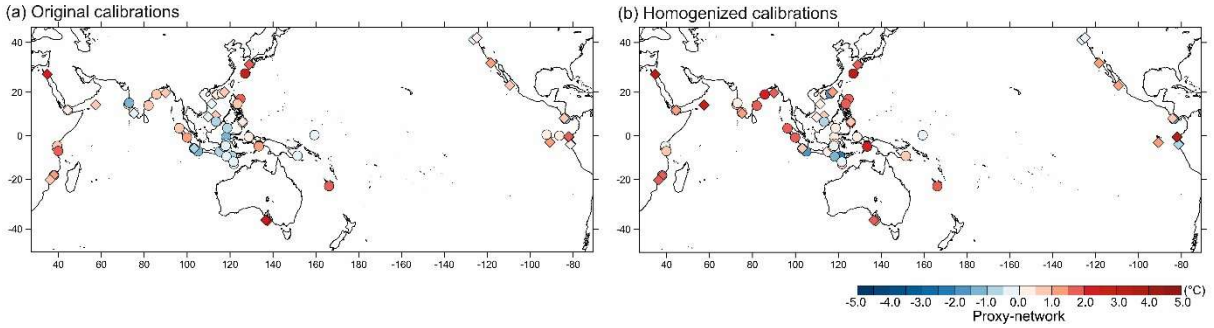

Fig. S2. Difference between Mg/Ca- (dots) and $U_{37}^{K'}$-(diamonds) based SST during the Common Era (CE) and the COBEv2 1850-1900 SST data. Colors indicate SSTs colder (blue) and warmer (red) than indicated by COBE.

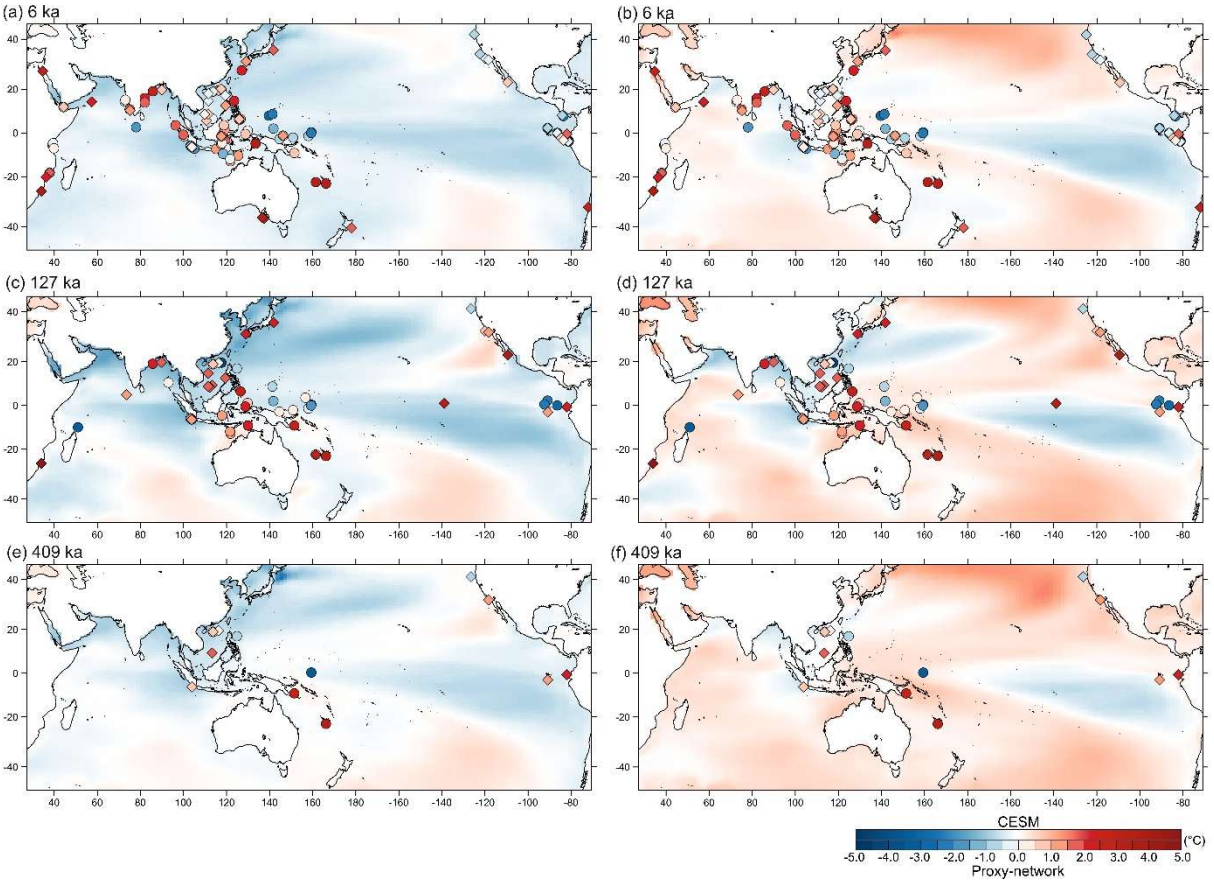

Fig. S3. Same as Fig. 2, but for homogenized SSTs. SST anomalies during (a, b) mid-Holocene, (c, d) MIS 5e, and (e, f) MIS 11c relative to the preindustrial period from Community Earth System Model (CESM) 1.2.2. time slice simulations without (a, c, e) and with (b, d, f) expanded NH vegetation. Symbols represent Mg/Ca- (dots) and $U_{37}^{K'}$-(diamonds) based SST anomalies relative to COBEv2 1850-1900 SST. Colors indicate SSTs colder (blue) and warmer (red) than the reference period.

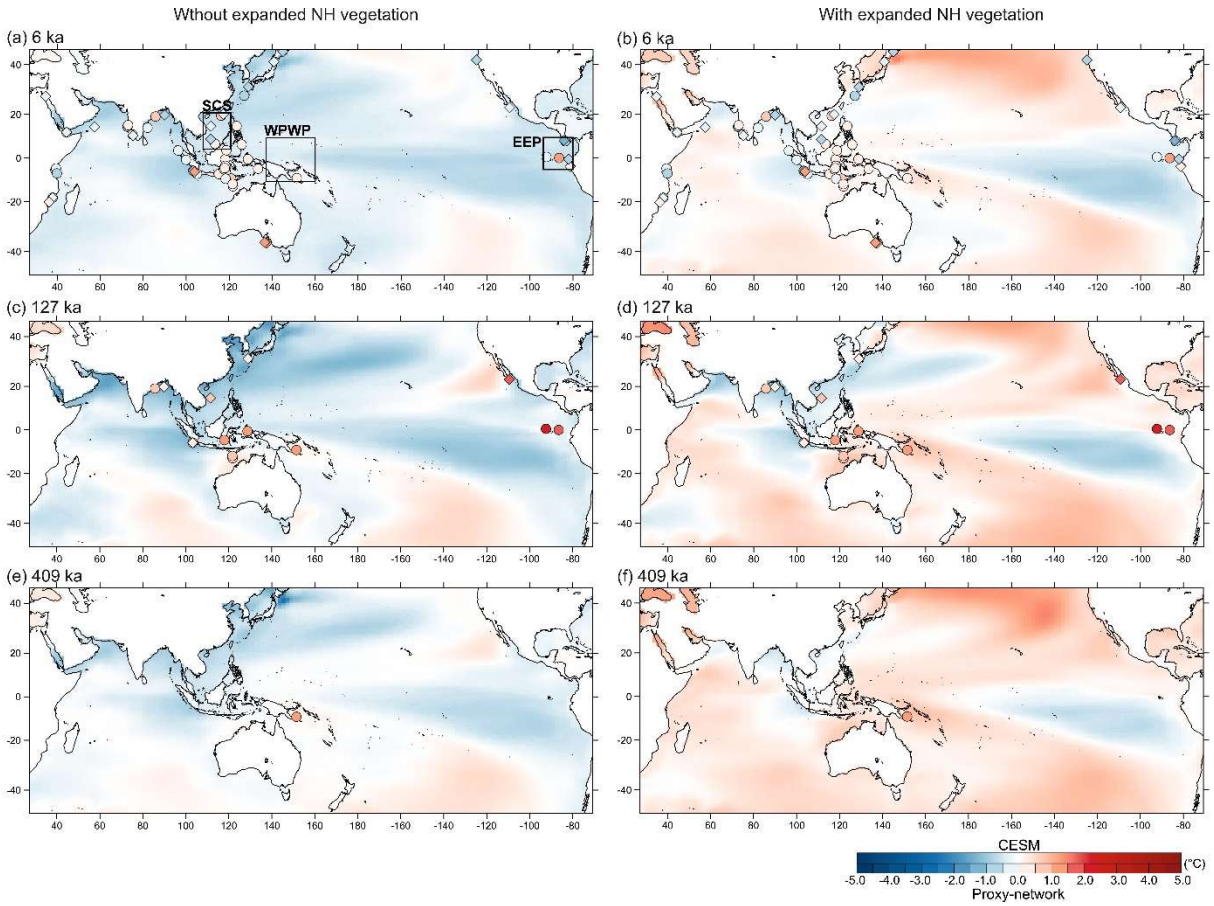

Fig. S4. Same as Fig. 2, but using reconstructed CE SSTs as preindustrial reference. SST anomalies during (a, b) mid-Holocene, (c, d) MIS 5e, and (e, f) MIS 11c relative to the preindustrial period from Community Earth System Model (CESM) 1.2.2. time slice simulations without (a, c, e) and with (b, d, f) expanded NH vegetation. Symbols represent Mg/Ca- (dots) and $U_{37}^{K'}$ -(diamonds) based SST anomalies relative to Common Era (CE) SST. Colors indicate SSTs colder (blue) and warmer (red) than the reference period.

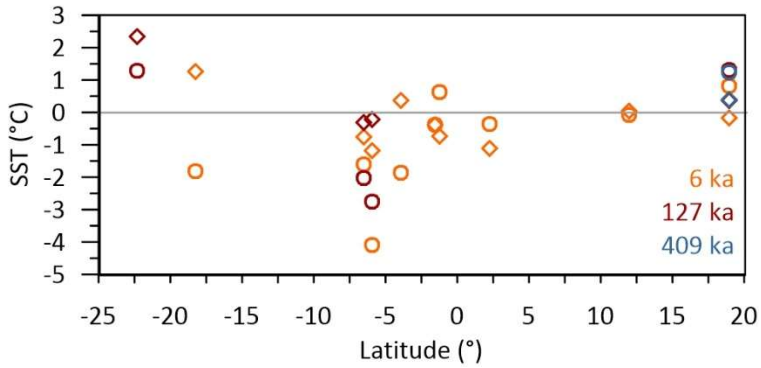

Fig. S5. Comparison of Mg/Ca- (dots) and $U_{37}^{K'}$-(diamonds) based SST anomalies from sites, where both proxy reconstructions are available for the 6-ka (orange), 127-ka (red) and 409-ka (blue) time slices.

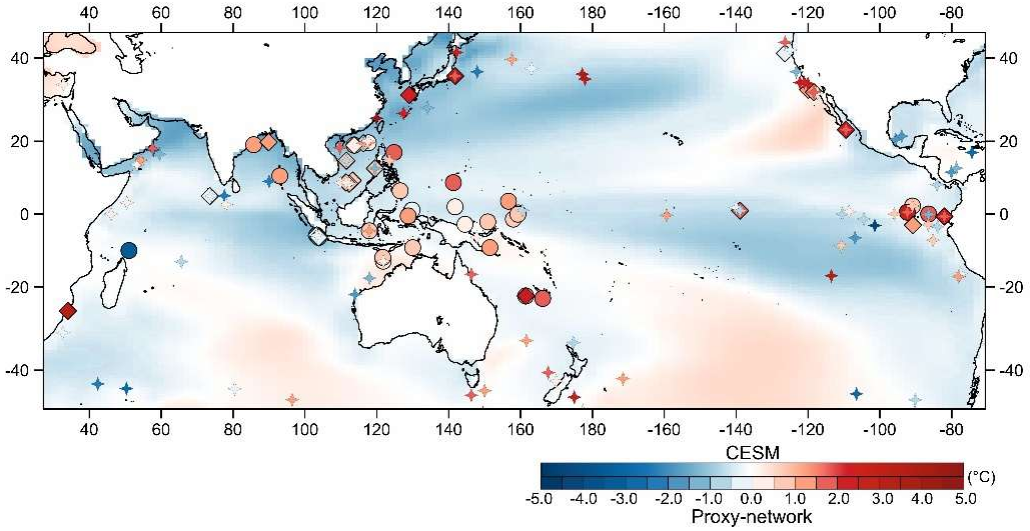

Fig. S6. Comparison of SST anomalies resulting from Mg/Ca and $U_{37}^{K'}$ (large dots and diamonds; this study) and SST anomalies resulting from Mg/Ca, $U_{37}^{K'}$ and microfossil assemblages (star-diamonds; Turney et al., 2020) during MIS 5e. The background map shows the SST anomalies in CESM (see main text).

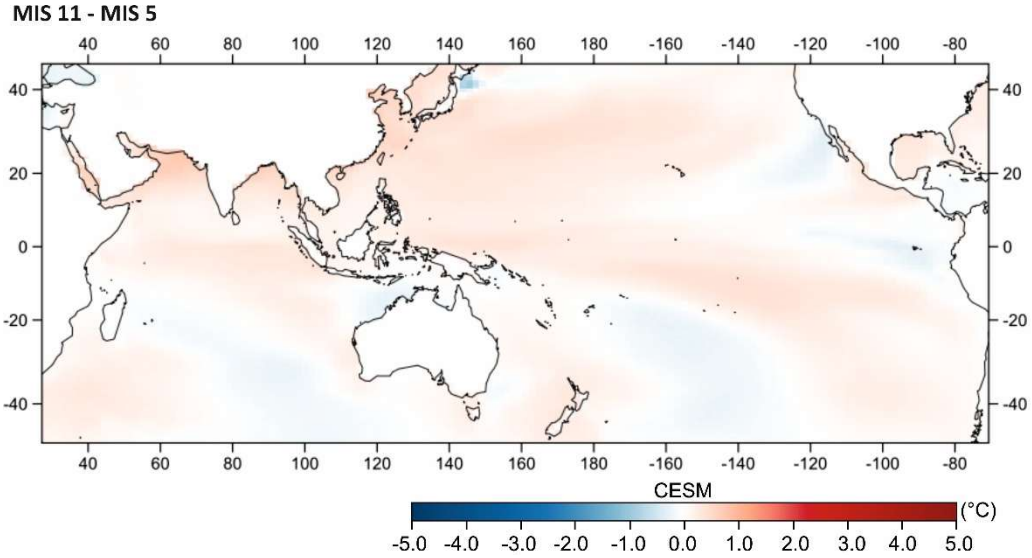

Fig. S7. Mean annual SST anomalies during MIS 11c relative to MIS 5e as derived from CESM time slice simulations. Colors indicate SSTs colder (blue) and warmer (red) than the reference period.

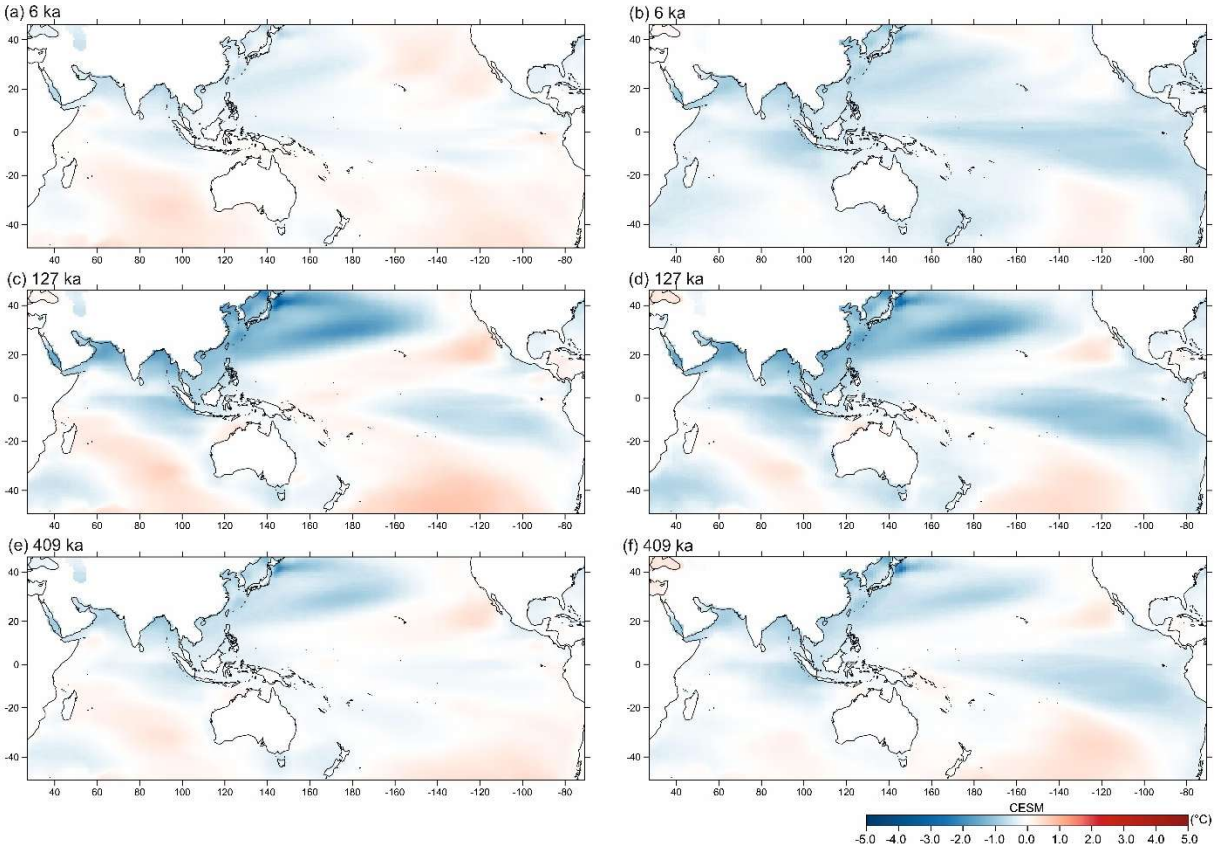

Fig. S8. Mean annual SST anomalies during (a, b) mid-Holocene, (c, d) MIS 5e, and (e, f) MIS 11c relative to the preindustrial period from CESM time slice simulations with fixed (a, c, e) and dynamic (b, d, f) greenhouse gases. Colors indicate SSTs colder (blue) and warmer (red) than the reference period.

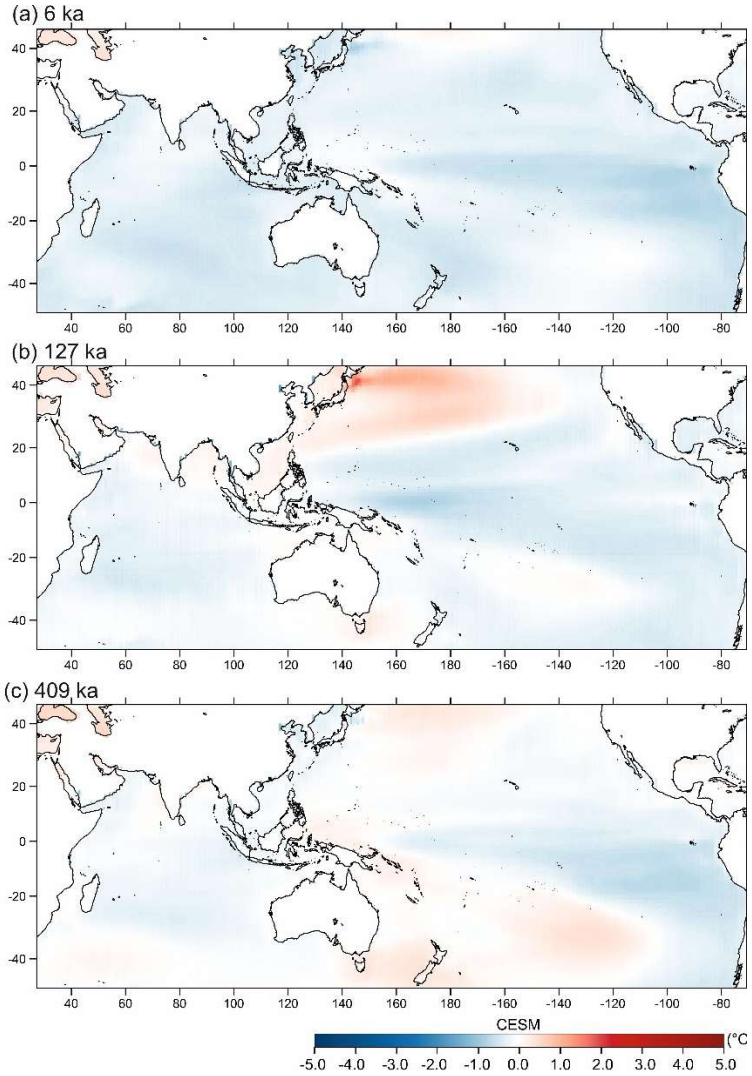

Fig. S9. Difference between mean annual SST anomalies with fixed and with dynamic greenhouse gas concentrations (calculated as SST anomalies with dynamic GHGs – SST anomalies with fixed GHGs) in CESM at (a) 6 ka, (b) 127 ka and (c) 409 ka.

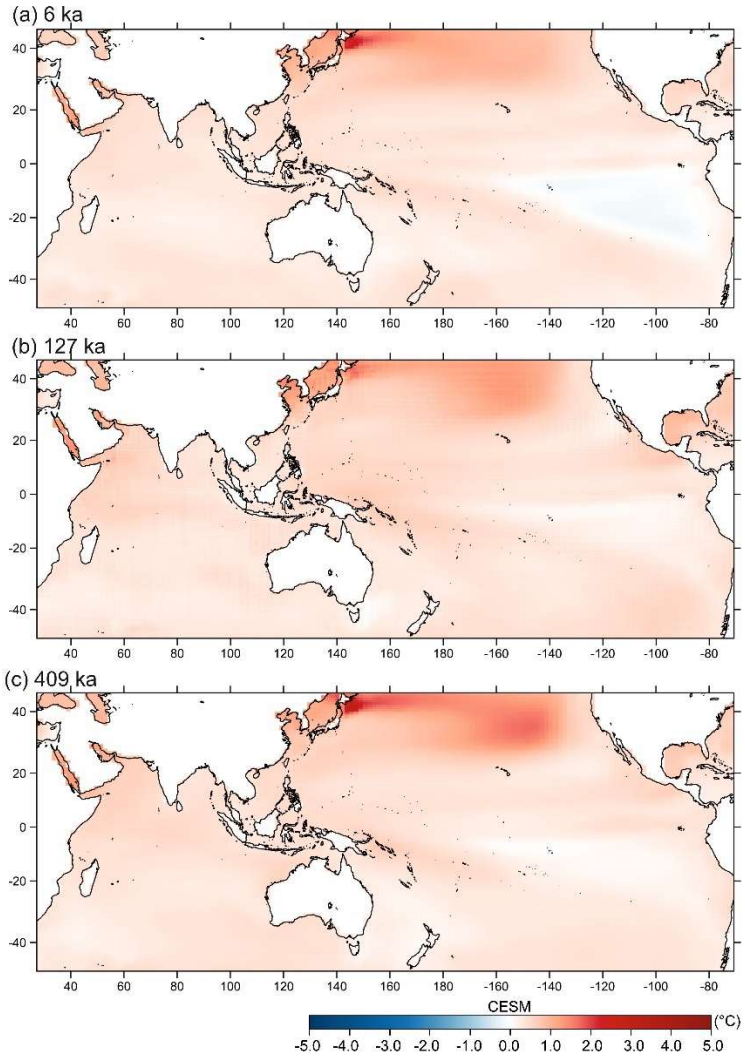

Fig. S10. Effect of vegetation expansion at (a) 6 ka, (b) 127 ka and (c) 409 ka. The vegetation effect was assessed by calculating the difference between mean annual SST anomalies derived from CESM runs with vegetation expansion and mean SST anomalies derived from CESM without vegetation expansion.

References

Anand, P., Kroon, D., Singh, A. D., Ganeshram, R. S., Ganssen, G., & Elderfield, H. (2008). Coupled sea surface temperature-seawaterδ18O reconstructions in the Arabian Sea at the millennial scale for the last 35 ka. *Paleoceanography, 23*(4). https://doi.org/10.1029/2007pa001564

Arz, H. W., Pätzold, J., Müller, P. J., & Moammar, M. O. (2003). Influence of Northern Hemisphere climate and global sea level rise on the restricted Red Sea marine environment during termination I. *Paleoceanography, 18*(2). https://doi.org/10.1029/2002PA000864

Barron, J. A., Heusser, L., Herbert, T., & Lyle, M. (2003). High-resolution climatic evolution of coastal northern California during the past 16,000 years. *Paleoceanography, 18*(1). https://doi.org/10.1029/2002pa000768

Benway, H. M., Mix, A. C., Haley, B. A., & Klinkhammer, G. P. (2006). Eastern Pacific Warm Pool paleosalinity and climate variability: 0–30 kyr. *Paleoceanography, 21*(3). https://doi.org/10.1029/2005pa001208

Bolliet, T., Holbourn, A., Kuhnt, W., Laj, C., Kissel, C., Beaufort, L., . . . Garbe-Schonberg, D. (2011). Mindanao Dome variability over the last 160 kyr: Episodic glacial cooling of the West Pacific Warm Pool. *Paleoceanography, 26*(1). https://doi.org/10.1029/2010pa001966

Bova, S. C., Herbert, T., Rosenthal, Y., Kalansky, J., Altabet, M., Chazen, C., . . . Zech, J. (2015). Links between eastern equatorial Pacific stratification and atmospheric CO2 rise during the last deglaciation. *Paleoceanography, 30*(11), 1407–1424. https://doi.org/10.1002/2015pa002816

Butzin, M., Köhler, P., & Lohmann, G. (2017). Marine Radiocarbon Reservoir Age Simulations for the Past 50,000 Years. *Geophysical Research Letters*. https://doi.org/10.1002/2017gl074688

Caley, T., Kim, J. H., Malaize, B., Giraudeau, J., Laepple, T., Caillon, N., . . . Damsté, J. S. (2011). High-latitude obliquity as a dominant forcing in the Agulhas current system *Climate of the Past, 7*(4), 1285–1296. https://doi.org/10.5194/cp-7-1285-2011

Cappelli, E. L. G., Holbourn, A., Kuhnt, W., & Regenberg, M. (2016). Changes in Timor Strait hydrology and thermocline structure during the past 130ka. *Palaeogeography Palaeoclimatology Palaeoecology, 462*, 112–124. https://doi.org/10.1016/j.palaeo.2016.09.010

Cheng, Z., Weng, C., Steinke, S., & Mohtadi, M. (2018). Anthropogenic modification of vegetated landscapes in southern China from 6,000 years ago. *Nature Geoscience*. https://doi.org/10.1038/s41561-018-0250-1

Clemens, S. C., Holbourn, A., Kubota, Y., Lee, K. E., Liu, Z., Chen, G., . . . Fox-Kemper, B. (2018). Precession-band variance missing from East Asian monsoon runoff. *Nat Commun, 9*(1), 3364. https://doi.org/10.1038/s41467-018-05814-0

Clemens, S. C., Yamamoto, M., Thirumalai, K., Giosan, L., Richey, J. N., Nilsson-Kerr, K., . . . McGrath, S. M. (2021). Remote and local drivers of Pleistocene South Asian summer monsoon precipitation: A test for future predictions. *Science Advances, 7*(23), eabg3848. https://doi.org/doi:10.1126/sciadv.abg3848

Dang, H., Jian, Z., Bassinot, F., Qiao, P., & Cheng, X. (2012). Decoupled Holocene variability in surface and thermocline water temperatures of the Indo-Pacific Warm Pool. *Geophysical Research Letters, 39*(1). https://doi.org/10.1029/2011gl050154

Dang, H., Jian, Z., Wang, Y., Mohtadi, M., Rosenthal, Y., Ye, L., . . . Kuhnt, W. (2020). Pacific warm pool subsurface heat sequestration modulated Walker circulation and ENSO activity during the Holocene. *Science Advances, 6*(42). https://doi.org/10.1126/sciadv.abc0402

De Deckker, P., Moros, M., Perner, K., Blanz, T., Wacker, L., Schneider, R., . . . Jansen, E. (2020). Climatic evolution in the Australian region over the last 94 ka - spanning human occupancy -, and unveiling the Last Glacial Maximum. *Quaternary Science Reviews, 249*. https://doi.org/10.1016/j.quascirev.2020.106593

de Garidel-Thoron, T., Beaufort, L., Linsley, B. K., & Dannenmann, S. (2001). Millennial-scale dynamics of the east Asian winter monsoon during the last 200,000 years. *Paleoceanography, 16*(5), 491–502. https://doi.org/10.1029/2000PA000557

de Garidel-Thoron, T., Rosenthal, Y., Bassinot, F., & Beaufort, L. (2005). Stable sea surface temperatures in the western Pacific warm pool over the past 1.75 million years. *Nature, 433*(7023), 294–298. https://doi.org/10.1038/nature03189

de Garidel-Thoron, T., Rosenthal, Y., Beaufort, L., Bard, E., Sonzogni, C., & Mix, A. C. (2007). A multiproxy assessment of the western equatorial Pacific hydrography during the last 30 kyr. *Paleoceanography, 22*, https://doi.org/10.1029/2006PA001269.

Dong, L., Li, L., Li, Q., Wang, H., & Zhang, C. L. (2015). Hydroclimate Implications of Thermocline Variability in the Southern South China Sea Over the Past 180,000 yr. *Quaternary Research, 83*(02), 370–377. https://doi.org/10.1016/j.yqres.2014.12.003

Dubois, N., & Kienast, M. (2011). Spatial reorganization in the equatorial divergence in the Eastern Tropical Pacific during the last 150 kyr. *Geophysical Research Letters, 38*(16). https://doi.org/10.1029/2011gl048325

Dubois, N., Kienast, M., Kienast, S., Normandeau, C., Calvert, S. E., Herbert, T. D., & Mix, A. (2011). Millennial-scale variations in hydrography and biogeochemistry in the Eastern Equatorial Pacific over the last 100 kyr. *Quaternary Science Reviews, 30*(1-2), 210–223. https://doi.org/10.1016/j.quascirev.2010.10.012

Dubois, N., Kienast, M., Normandeau, C., & Herbert, T. D. (2009). Eastern equatorial Pacific cold tongue during the Last Glacial Maximum as seen from alkenone paleothermometry. *Paleoceanography, 24*(4). https://doi.org/10.1029/2009pa001781

Dyez, K. A., Ravelo, A. C., & Mix, A. C. (2016). Evaluating drivers of Pleistocene eastern tropical Pacific sea surface temperature. *Paleoceanography, 31*(8), 1054–1069. https://doi.org/10.1002/2015PA002873

Etourneau, J., Schneider, R., Blanz, T., & Martinez, P. (2010). Intensification of the Walker and Hadley atmospheric circulations during the Pliocene–Pleistocene climate transition. *Earth and Planetary Science Letters, 297*(1), 103–110. https://doi.org/10.1016/j.epsl.2010.06.010

Fan, W., Jian, Z., Chu, Z., Dang, H., Wang, Y., Bassinot, F., . . . Bian, Y. (2018). Variability of the Indonesian Throughflow in the Makassar Strait over the Last 30 ka. *Sci Rep, 8*(1), 5678. https://doi.org/10.1038/s41598-018-24055-1

Fan, W., Jian, Z. M., Bassinot, F., & Chu, Z. H. (2013). Holocene centennial-scale changes of the Indonesian and South China Sea throughflows: Evidences from the Makassar Strait. *Global and Planetary Change, 111*, 111–117. https://doi.org/10.1016/j.gloplacha.2013.08.017

Fraser, N., Kuhnt, W., Holbourn, A., Bolliet, T., Andersen, N., Blanz, T., & Beaufort, L. (2014). Precipitation variability within the West Pacific Warm Pool over the past 120 ka: Evidence from the Davao Gulf, southern Philippines. *Paleoceanography, 29*(11), 1094–1110. https://doi.org/10.1002/2013pa002599

Gibbons, F. T., Oppo, D. W., Mohtadi, M., Rosenthal, Y., Cheng, J., Liu, Z., & Linsley, B. K. (2014). Deglacial δ18O and hydrologic variability in the tropical Pacific and Indian Oceans. *Earth and Planetary Science Letters, 387*, 240–251. https://doi.org/10.1016/j.epsl.2013.11.032

Govil, P., & Naidu, D. P. (2011). Variations of Indian monsoon precipitation during the last 32kyr reflected in the surface hydrography of the Western Bay of Bengal. *Quaternary Science Reviews, 30*(27), 3871–3879. https://doi.org/10.1016/j.quascirev.2011.10.004

Govil, P., & Naidu, P. D. (2010). Evaporation-precipitation changes in the eastern Arabian Sea for the last 68 ka: Implications on monsoon variability. *Paleoceanography, 25*(1). https://doi.org/10.1029/2008pa001687

Gray, W. R., Weldeab, S., Lea, D. W., Rosenthal, Y., Gruber, N., Donner, B., & Fischer, G. (2018). The effects of temperature, salinity, and the carbonate system on Mg/Ca in Globigerinoides ruber (white): A global sediment trap calibration. *Earth and Planetary Science Letters, 482*, 607–620. https://doi.org/10.1016/j.epsl.2017.11.026

Harada, N., Ahagon, N., Sakamoto, T., Uchida, M., Ikehara, M., & Shibata, Y. (2006). Rapid fluctuation of alkenone temperature in the southwestern Okhotsk Sea during the past 120 ky. *Global and Planetary Change, 5329-46*. https://doi.org/10.1016/j.gloplacha.2006.01.010

Hendrizan, M., Kuhnt, W., & Holbourn, A. (2017). Variability of Indonesian Throughflow and Borneo Runoff During the Last 14 kyr. *Paleoceanography, 32*(10), 1054–1069. https://doi.org/10.1002/2016pa003030

Herbert, T. D., Cleaveland Peterson, L., Lawrence, K. T., & Liu, Z. (2010). Tropical Ocean Temperatures Over the Past 3.5 Million Years. *Science, 328*, 1530–1534. https://doi.org/10.1126/science.1185435

Herbert, T. D., Schuffert, J. D., Andreasen, D., Heusser, L., Lyle, M., Mix, A., . . . Herguera, J. C. (2001). Collapse of the California Current during glacial maxima linked to climate change on land. *Science, 293*(5527), 71–76. https://doi.org/10.1126/science.1059209

Herbert, T. D., Schuffert, J. D., Thomas, D., Lange, C., Weinheimer, A., Peleo-Alampay, A., & Herguera, J.-C. (1998). Depth and seasonality of alkenone production along the California Margin inferred from a core top transect. *Paleoceanography, 13*(3), 263–271. https://doi.org/10.1029/98PA00069

Heusser, L., Lyle, M., & Mix, A. (2000). Vegetation and climate of the northwest coast of North America during the last 500 K.Y.: High-resolution pollen evidence from the northern California margin. *Proceedings of the Ocean Drilling Program: Scientific results, 167*. https://doi.org/10.2973/odp.proc.sr.167.206.2000

Holbourn, A., Kuhnt, W., Kawamura, H., Jian, Z., Grootes, P., Erlenkeuser, H., & Xu, J. (2005). Orbitally paced paleoproductivity variations in the Timor Sea and Indonesian Throughflow variability during the last 460 kyr. *Paleoceanography, 20*(3), https://doi.org/10.1029/2004pa001094

Hollstein, M., Mohtadi, M., Kienast, M., Rosenthal, Y., Groeneveld, J., Oppo, D. W., . . . Lückge, A. (2020). The Impact of Astronomical Forcing on Surface and Thermocline Variability Within the Western Pacific Warm Pool Over the Past 160 kyr. *Paleoceanography and Paleoclimatology, 35*(6). https://doi.org/10.1029/2019pa003832

Huang, C.-Y., Wu, S.-F., Zhao, M., Chen, M.-T., Wang, C.-H., Tu, X., & Yuan, P. B. (1997). Surface ocean and monsoon climate variability in the South China Sea since the last glaciation. *Marine Micropaleontology, 32*(1), 71–94. https://doi.org/10.1016/S0377-8398(97)00014-5

Huang, E., Chen, Y. C., Schefuß, E., Steinke, S., Liu, J., Tian, J., . . . Mohtadi, M. (2018). Precession and glacial-cycle controls of monsoon precipitation isotope changes over East Asia during the Pleistocene. *Earth and Planetary Science Letters, 494*, 1–11. https://doi.org/10.1016/j.epsl.2018.04.046

Jasper, J. P., Hayes, J. M., Mix, A. C., & Prahl, F. G. (1994). Photosynthetic fractionation of 13C and concentrations of dissolved CO2 in the central equatorial Pacific during the last 255,000 years. *Paleoceanography, 9*(6), 781–798. https://doi.org/10.1029/94PA02116

Jia, Q., Li, T., Xiong, Z., Steinke, S., Jiang, F., Chang, F., & Qin, B. (2018). Hydrological variability in the western tropical Pacific over the past 700 kyr and its linkage to Northern Hemisphere climatic change. *Palaeogeography, Palaeoclimatology, Palaeoecology*. https://doi.org/10.1016/j.palaeo.2017.12.039

Jian, Z., Wang, Y., Dang, H., Lea, D. W., Liu, Z., Jin, H., & Yin, Y. (2020). Half-precessional cycle of thermocline temperature in the western equatorial Pacific and its bihemispheric dynamics. *Proc Natl Acad Sci U S A, 117*(13), 7044–7051. https://doi.org/10.1073/pnas.1915510117

Jian, Z., Wang, Y., Dang, H., Mohtadi, M., Rosenthal, Y., Lea, D. W., . . . Wang, X. (2022). Warm pool ocean heat content regulates ocean–continent moisture transport. *Nature, 612*, 92–99. https://doi.org/10.1038/s41586-022-05302-y

Johnstone, H. J. H., Kiefer, T., Elderfield, H., & Schulz, M. (2014). Calcite saturation, foraminiferal test mass, and Mg/Ca-based temperatures dissolution corrected using XDX—A 150 ka record from the western Indian Ocean. *Geochemistry, Geophysics, Geosystems, 15*(3), 781–797. https://doi.org/10.1002/2013GC004994

Jonkers, L., Hollstein, M., Siccha, M., & Kucera, M. (accepted). The PALMOD 130k marine palaeoclimate data synthesis version 2. *Earth System Science Data*.

Kawahata, H., Yamamoto, H., Ohkushi, K. i., Yokoyama, Y., Kimoto, K., Ohshima, H., & Matsuzaki, H. (2009). Changes of environments and human activity at the Sannai-Maruyama ruins in Japan during the mid-Holocene Hypsithermal climatic interval. *Quaternary Science Reviews, 28*(9), 964–974. https://doi.org/10.1016/j.quascirev.2008.12.009

Kiefer, T., McCave, I. N., & Elderfield, H. (2006). Antarctic control on tropical Indian Ocean sea surface temperature and hydrography. *Geophysical Research Letters, 33*(24). https://doi.org/10.1029/2006gl027097

Kienast, M., Kienast, S. S., Calvert, S. E., Eglinton, T. I., Mollenhauer, G., Francois, R., & Mix, A. C. (2006). Eastern Pacific cooling and Atlantic overturning circulation during the last deglaciation. *Nature, 443*(7113), 846–849. https://doi.org/10.1038/nature05222

Kim, J.-H., Rimbu, N., Lorenz, S. J., Lohmann, G., Nam, S.-I., Schouten, S., . . . Schneider, R. R. (2004). North Pacific and North Atlantic sea-surface temperature variability during the Holocene. *Quaternary Science Reviews, 23*(20-22), 2141–2154. https://doi.org/10.1016/j.quascirev.2004.08.010

Kim, J.-H., Schneider, R. R., Hebbeln, D., Müller, P. J., & Wefer, G. (2002). Last deglacial sea-surface temperature evolution in the Southeast Pacific compared to climate changes on the South American continent. *Quaternary Science Reviews, 21*(18), 2085–2097. https://doi.org/10.1016/S0277-3791(02)00012-4

Koutavas, A., & Sachs, J. P. (2008). Northern timing of deglaciation in the eastern equatorial Pacific from alkenone paleothermometry. *Paleoceanography, 23*(4), https://doi.org/10.1029/2008pa001593

Kuhnert, H., Kuhlmann, H., Mohtadi, M., Meggers, H., Baumann, K.-H., & Pätzold, J. (2014). Holocene tropical western Indian Ocean sea surface temperatures in covariation with climatic changes in the Indonesian region. *Paleoceanography, 29*(5), 423–437. https://doi.org/10.1002/2013pa002555

Lauterbach, S., Andersen, N., Wang, Y. V., Blanz, T., Larsen, T., & Schneider, R. R. (2020). An ~130 kyr Record of Surface Water Temperature and δ18O From the Northern Bay of Bengal: Investigating the Linkage Between Heinrich Events and Weak Monsoon Intervals in Asia. *Paleoceanography and Paleoclimatology, 35*(2), e2019PA003646. https://doi.org/10.1029/2019PA003646

Lawrence, K. T., Liu, Z., & Herbert, T. D. (2006). Evolution of the Eastern Tropical Pacific Through Plio-Pleistocene Glaciation. *Science, 312*(5770), 79–83. doi:10.1126/science.1120395

Lea, D. W., Pak, D. K., Belanger, C. L., Spero, H. J., Hall, M. A., & Shackleton, N. J. (2006). Paleoclimate history of Galápagos surface waters over the last 135,000yr. *Quaternary Science Reviews, 25*(11-12), 1152–1167. https://doi.org/10.1016/j.quascirev.2005.11.010

Lea, D. W., Pak, D. K., & Spero, H. J. (2000). Climate impact of late quaternary equatorial pacific sea surface temperature variations. *Science, 289*(5485), 1719–1724.

Leduc, G., Vidal, L., Tachikawa, K., Rostek, F., Sonzogni, C., Beaufort, L., & Bard, E. (2007). Moisture transport across Central America as a positive feedback on abrupt climatic changes. *Nature, 445*(7130), 908–911. https://doi.org/10.1038/nature05578

Levi, C., Labeyrie, L., Bassinot, F., Guichard, F., Cortijo, E., Waelbroeck, C., . . . Elderfield, H. (2007). Low-latitude hydrological cycle and rapid climate changes during the last deglaciation. *Geochemistry, Geophysics, Geosystems, 8*(5). https://doi.org/10.1029/2006gc001514

Li, L., Li, Q., Tian, J., Wang, P., Wang, H., & Liu, Z. (2011). A 4-Ma record of thermal evolution in the tropical western Pacific and its implications on climate change. *Earth and Planetary Science Letters, 309*(1-2), 10–20. https://doi.org/10.1016/j.epsl.2011.04.016

Linsley, B. K., Rosenthal, Y., & Oppo, D. W. (2010). Holocene evolution of the Indonesian throughflow and the western Pacific warm pool. *Nature Geoscience, 3*(8), 578–583. https://doi.org/10.1038/Ngeo920

Lisiecki, L. E., & Stern, J. V. (2016). Regional and global benthic $\delta^{18}O$ stacks for the last glacial cycle. *Paleoceanography, 31*(10), 1368–1394. https://doi.org/10.1002/2016pa003002

Lo, L., Chang, S. P., Wei, K. Y., Lee, S. Y., Ou, T. H., Chen, Y. C., . . . Shen, C. C. (2017). Nonlinear climatic sensitivity to greenhouse gases over past 4 glacial/interglacial cycles. *Sci Rep, 7*(1), 4626. https://doi.org/10.1038/s41598-017-04031-x

Lo, L., Shen, C.-C., Zeeden, C., Tsai, Y.-H., Yin, Q., Yang, C.-C., . . . Chen, Y.-C. (2022). Orbital control on the thermocline structure during the past 568 kyr in the Solomon Sea, southwest equatorial Pacific. *Quaternary Science Reviews, 295*. https://doi.org/10.1016/j.quascirev.2022.107756

Lo, L., Shen, C. C., Wei, K. Y., Burr, G. S., Mii, H. S., Chen, M. T., . . . Tsai, M. C. (2014). Millennial meridional dynamics of the Indo-Pacific Warm Pool during the last termination. *Climate of the Past, 10*(6), 2253–2261. https://doi.org/10.5194/cp-10-2253-2014

Lopes dos Santos, R. A., Spooner, M. I., Barrows, T. T., De Deckker, P., Damsté, J. S., & Schouten, S. (2013). Comparison of organic (UK'37, TEXH86, LDI) and faunal proxies (foraminiferal assemblages) for reconstruction of late Quaternary sea surface temperature variability from offshore southeastern Australia. *Paleoceanography, 28*, 377–387. https://doi.org/10.1002/palo.20035

Lückge, A., Mohtadi, M., Rühlemann, C., Scheeder, G., Vink, A., Reinhardt, L., & Wiedicke, M. (2009). Monsoon versus ocean circulation controls on paleoenvironmental condition off southern Sumatra during the past 300,000 years. *Paleoceanography, 24*. https://doi.org/10.1029/2008PA001627

Medina-Elizalde, M., & Lea, D. W. (2005). The Mid-Pleistocene Transition in the Tropical Pacific. *Science, 310*, 1009–1012. 10.1126/science.111593

Mohtadi, M., Lückge, A., Steinke, S., Groeneveld, J., Hebbeln, D., & Westphal, N. (2010). Late Pleistocene surface and thermocline conditions of the eastern tropical Indian Ocean. *Quaternary Science Reviews, 29*(7-8), 887–896. https://doi.org/10.1016/j.quascirev.2009.12.006

Mohtadi, M., Prange, M., Oppo, D. W., De Pol-Holz, R., Merkel, U., Zhang, X., . . . Luckge, A. (2014). North Atlantic forcing of tropical Indian Ocean climate. *Nature, 509*(7498), 76–80. https://doi.org/10.1038/nature13196

Mohtadi, M., Romero, O. E., Kaiser, J., & Hebbeln, D. (2007). Cooling of the southern high latitudes during the Medieval Period and its effect on ENSO. *Quaternary Science Reviews, 26*(7), 1055–1066. https://doi.org/10.1016/j.quascirev.2006.12.008

Mohtadi, M., Steinke, S., Lückge, A., Groeneveld, J., & Hathorne, E. C. (2010). Glacial to Holocene surface hydrography of the tropical eastern Indian Ocean. *Earth and Planetary Science Letters, 292*(1-2), 89–97. https://doi.org/10.1016/j.epsl.2010.01.024

Naidu, P. D., & Govil, P. (2010). New evidence on the sequence of deglacial warming in the tropical Indian Ocean. *Journal of Quaternary Science, 25*(7), 1138–1143. https://doi.org/10.1002/jqs.1392

Newton, A., Thunell, R., & Stott, L. (2006). Climate and hydrographic variability in the Indo-Pacific Warm Pool during the last millennium. *Geophysical Research Letters, 33*(19). https://doi.org/10.1029/2006GL027234

Nilsson-Kerr, K., Anand, P., Holden, P. B., Clemens, S. C., & Leng, M. J. (2021). Dipole patterns in tropical precipitation were pervasive across landmasses throughout Marine Isotope Stage 5. *Communications Earth & Environment, 2*(1), 64. https://doi.org/10.1038/s43247-021-00133-7

Nilsson-Kerr, K., Anand, P., Sexton, P. F., Leng, M. J., & Naidu, P. D. (2022). Indian Summer Monsoon variability 140–70 thousand years ago based on multi-proxy records from the Bay of Bengal. *Quaternary Science Reviews, 279*. https://doi.org/10.1016/j.quascirev.2022.107403

Nürnberg, D., Böschen, T., Doering, K., Mollier-Vogel, E., Raddatz, J., & Schneider, R. (2015). Sea surface and subsurface circulation dynamics off equatorial Peru during the last ~17 kyr. *Paleoceanography, 30*(7), 984–999. https://doi.org/10.1002/2014PA002706

Oppo, D. W., Linsley, B. K., Rosenthal, Y., Dannenmann, S., & Beaufort, L. (2003). Orbital and suborbital climate variability in the Sulu Sea, western tropical Pacific. *Geochemistry, Geophysics, Geosystems, 4*(1), 1–20. https://doi.org/10.1029/2001gc000260

Pahnke, K., & Sachs, J. P. (2006). Sea surface temperatures of southern midlatitudes 0-160 kyr B.P. *Paleoceanography, 21*(2), https://doi.org/10.1029/2005pa001191

Panmei, C., Naidu, P. D., & Mohtadi, M. (2017). Bay of Bengal Exhibits Warming Trend During the Younger Dryas: Implications of AMOC. *Geochemistry Geophysics Geosystems, 18*(12), 4317–4325. https://doi.org/10.1002/2017GC007075

Pelejero, C., Grimalt, J. O., Heilig, S., Kienast, M., & Wang, L. (1999). High-resolution UK37temperature reconstructions in the South China Sea over the past 220 kyr. *Paleoceanography, 14*(2), 224–231. https://doi.org/10.1029/1998pa900015

Pena, L. D., Cacho, I., Ferretti, P., & Hall, M. A. (2008). El Niño-Southern Oscillation-like variability during glacial terminations and interlatitudinal teleconnections. *Paleoceanography, 23*(3), n/a–n/a. https://doi.org/10.1029/2008pa001620

Reimer, P. J., Austin, W. E. N., Bard, E., Bayliss, A., Blackwell, P. G., Bronk Ramsey, C., . . . Talamo, S. (2020). The IntCal20 Northern Hemisphere Radiocarbon Age Calibration Curve (0–55 cal kBP). *Radiocarbon, 62*(4), 725–757. https://doi.org/10.1017/rdc.2020.41

Rincón-Martínez, D., Lamy, F., Contreras, S., Leduc, G., Bard, E., Saukel, C., . . . Tiedemann, R. (2010). More humid interglacials in Ecuador during the past 500 kyr linked to latitudinal shifts of the equatorial front and the Intertropical Convergence Zone in the eastern tropical Pacific. *Paleoceanography, 25*(2). https://doi.org/10.1029/2009PA001868

Rippert, N., Baumann, K.-H., & PÄTzold, J. (2015). Thermocline fluctuations in the western tropical Indian Ocean during the past 35 ka. *Journal of Quaternary Science, 30*(3), 201–210. https://doi.org/10.1002/jqs.2767

Romahn, S., Mackensen, A., Groeneveld, J., & Pätzold, J. (2014). Deglacial intermediate water reorganization: new evidence from the Indian Ocean. *Climate of the Past, 10*(1), 293–303. 10.5194/cp-10-293-2014

Rostek, F., Bard, E., Beaufort, L., Sonzogni, C., & Ganssen, G. (1997). Sea surface temperature and productivity records for the past 240 kyr in the Arabian Sea. *Deep Sea Research Part II: Topical Studies in Oceanography, 44*(6-7), 1461–1480. https://doi.org/10.1016/S0967-0645(97)00008-8

Russon, T., Elliot, M., Sadekov, A., Cabioch, G., Corrège, T., & De Deckker, P. (2011). The mid-Pleistocene transition in the subtropical southwest Pacific. *Paleoceanography, 26*(1). 10.1029/2010pa002019

Sadatzki, H., Sarnthein, M., & Andersen, N. (2016). Changes in monsoon-driven upwelling in the South China Sea over glacial Terminations I and II: a multi-proxy record. *International Journal of Earth Sciences, 105*(4), 1273–1285. https://doi.org/10.1007/s00531-015-1227-6

Sagawa, T., Yokoyama, Y., Ikehara, M., & Kuwae, M. (2012). Shoaling of the western equatorial Pacific thermocline during the last glacial maximum inferred from multispecies temperature reconstruction of planktonic foraminifera. *Palaeogeography, Palaeoclimatology, Palaeoecology, 346–347*, 120–129. https://doi.org/10.1016/j.palaeo.2012.06.002

Saikku, R., Stott, L., & Thunell, R. (2009). A bi-polar signal recorded in the western tropical Pacific: Northern and Southern Hemisphere climate records from the Pacific warm pool during the last Ice Age. *Quaternary Science Reviews, 28*(23-24), 2374–2385. https://doi.org/10.1016/j.quascirev.2009.05.007

Saraswat, R., Lea, D. W., Nigam, R., Mackensen, A., & Naik, D. K. (2013). Deglaciation in the tropical Indian Ocean driven by interplay between the regional monsoon and global teleconnections. *Earth and Planetary Science Letters, 375*, 166–175. https://doi.org/10.1016/j.epsl.2013.05.022

Saraswat, R., Nigam, R., Weldeab, S., Mackensen, A., & Naidu, P. D. (2005). A first look at past sea surface temperatures in the equatorial Indian Ocean from Mg/Ca in foraminifera. *Geophysical Research Letters, 32*(24). https://doi.org/10.1029/2005gl024093

Schröder, J. F., Holbourn, A., Kuhnt, W., & Küssner, K. (2016). Variations in sea surface hydrology in the southern Makassar Strait over the past 26 kyr. *Quaternary Science Reviews, 154*, 143–156. https://doi.org/10.1016/j.quascirev.2016.10.018

Schröder, J. F., Kuhnt, W., Holbourn, A., Beil, S., Zhang, P., Hendrizan, M., & Xu, J. (2018). Deglacial Warming and Hydroclimate Variability in the Central Indonesian Archipelago. *Paleoceanography and Paleoclimatology*. https://doi.org/10.1029/2018pa003323

Setiawan, R. Y., Mohtadi, M., Southon, J., Groeneveld, J., Steinke, S., & Hebbeln, D. (2015). The consequences of opening the Sunda Strait on the hydrography of the eastern tropical Indian Ocean. *Paleoceanography, 30*(10), 1358–1372. https://doi.org/10.1002/2015pa002802

Shiau, L. J., Yu, P. S., Wei, K. Y., Yamamoto, M., Lee, T. Q., Fang, T. H., & Chen, M. T. (2008). Sea surface temperature, productivity, and terrestrial flux variations of the southeastern South China Sea over the past 800000 years (IMAGES MD972142). *Terrestrial, Atmospheric and Oceanic Sciences, 19*, 363–376. 10.3319/TAO.2008.19.4.363(IMAGES)

Sonzogni, C., Bard, E., & Rostek, F. (1998). Tropical sea-surface temperatures during the last glacial period: A view based on alkenones in Indian Ocean sediments. *Quaternary Science Reviews, 17*(12), 1185–1201.

Steinke, S., Glatz, C., Mohtadi, M., Groeneveld, J., Li, Q., & Jian, Z. (2011). Past dynamics of the East Asian monsoon: No inverse behaviour between the summer and winter monsoon during the Holocene. *Global and Planetary Change, 78*(3-4), 170–177. https://doi.org/10.1016/j.gloplacha.2011.06.006

Steinke, S., Kienast, M., Groeneveld, J., Lin, L.-C., Chen, M.-T., & Rendle-Bühring, R. (2008). Proxy dependence of the temporal pattern of deglacial warming in the tropical South China Sea: toward resolving seasonality. *Quaternary Science Reviews, 27*(7-8), 688–700. 10.1016/j.quascirev.2007.12.003

Steinke, S., Kienast, M., Pflaumann, U., Weinelt, M., & Stattegger, K. (2001). A High-Resolution Sea-Surface Temperature Record from the Tropical South China Sea (16,500–3000 yr B.P.). *Quaternary Research, 55*(3), 352–362. https://doi.org/10.1006/qres.2001.2235

Stott, L., Cannariato, K., Thunell, R., Haug, G. H., Koutavas, A., & Lund, S. (2004). Decline of surface temperature and salinity in the western tropical Pacific Ocean in the Holocene epoch. *Nature 431*, 56–59.

Stott, L., Poulsen, C. J., Lund, D. C., & Thunell, R. (2002). Super ENSO and global climate oscillations at millennial time scales. *Science, 297*, 222–229.

Stott, L., Timmermann, A., & Thunell, R. (2007). Southern Hemisphere and deep-sea warming led deglacial atmospheric CO_2 rise and tropical warming. *Science, 318*(5849), 435–438. https://doi.org/10.1126/science.1143791

Sun, Y., Oppo, D. W., Xiang, R., Liu, W., & Gao, S. (2005). Last deglaciation in the Okinawa Trough: Subtropical northwest Pacific link to Northern Hemisphere and tropical climate. *Paleoceanography, 20*(4), https://doi.org/.1029/2004pa001061

Tachikawa, K., Timmermann, A., Vidal, L., Sonzogni, C., & Timm, O. E. (2014). CO_2 radiative forcing and Intertropical Convergence Zone influences on western Pacific warm pool climate over the past 400 ka. *Quaternary Science Reviews, 86*(0), 24–34. https://doi.org/10.1016/j.quascirev.2013.12.018

Tachikawa, K., Vidal, L., Sonzogni, C., & Bard, E. (2009). Glacial/interglacial sea surface temperature changes in the Southwest Pacific ocean over the past 360ka. *Quaternary Science Reviews, 28*(13-14), 1160–1170. https://doi.org/10.1016/j.quascirev.2008.12.013

Tierney, J. E., Pausata, F. S. R., & deMenocal, P. (2016). Deglacial Indian monsoon failure and North Atlantic stadials linked by Indian Ocean surface cooling. *Nature Geoscience, 9*(1), 46–50. https://doi.org/10.1038/ngeo2603

Tierney, J. E., & Tingley, M. P. (2018). BAYSPLINE: A New Calibration for the Alkenone Paleothermometer. *Paleoceanography and Paleoclimatology, 33*, 281–301. https://doi.org/10.1002/2017PA003201

Turney, C. S. M., Jones, R. T., McKay, N. P., Van Sebille, E., Thomas, Z., Hillenbrand, C.-D., & Fogwill, C. J. (2020). A global mean sea surface temperature dataset for the Last Interglacial (129–116 ka) and contribution of thermal expansion to sea level change. *Earth System Science Data, 12*, 3341–3356. https://doi.org/10.5194/essd-12-3341-2020

Wang, L., Sarnthein, M., Erlenkeuser, H., Grimalt, J. O., Grootes, P. M., Heilig, S., . . . Pflaumann, U. (1999). East Asian monsoon climate during the Late Pleistocene: high-resolution sediment records from the South China Sea. *Marine Geology, 156*(1-4), 245–284. https://doi.org/10.1016/S0025-3227(98)00182-0

Wang, X., Jian, Z., Lückge, A., Wang, Y., Dang, H., & Mohtadi, M. (2018). Precession-paced thermocline water temperature changes in response to upwelling conditions off southern Sumatra over the past 300,000 years. *Quaternary Science Reviews, 192*, 123–134. https://doi.org/10.1016/j.quascirev.2018.05.035

Wang, Y. V., Leduc, G., Regenberg, M., Andersen, N., Larsen, T., Blanz, T., & Schneider, R. R. (2013). Northern and southern hemisphere controls on seasonal sea surface temperatures in the Indian Ocean during the last deglaciation. *Paleoceanography, 28*(4), 619–632. https://doi.org/10.1002/palo.20053

Weiss, T. L., Linsley, B. K., Gordon, A. L., Rosenthal, Y., & Dannenmann-Di Palma, S. (2022). Constraints on Marine Isotope Stage 3 and 5 Sea Level From the Flooding History of the Karimata Strait in Indonesia. *Paleoceanography and Paleoclimatology, 37*(9), e2021PA004361. https://doi.org/10.1029/2021PA004361

Windler, G., Tierney, J. E., Di Nezio, P. N., Gibson, K., & Thunell, R. (2019). Shelf exposure influence on Indo-Pacific Warm Pool climate for the last 450,000 years. *Earth and Planetary Science Letters, 516*, 66–76. https://doi.org/10.1016/j.epsl.2019.03.038

Xu, J., Holbourn, A., Kuhnt, W., Jian, Z., & Kawamura, H. (2008). Changes in the thermocline structure of the Indonesian outflow during Terminations I and II. *Earth and Planetary Science Letters, 273*(1-2), 152–162. https://doi.org/10.1016/j.epsl.2008.06.029

Xu, J., Kuhnt, W., Holbourn, A., Andersen, N., & Bartoli, G. (2006). Changes in the vertical profile of the Indonesian Throughflow during Termination II: Evidence from the Timor Sea. *Paleoceanography, 21*(4). https://doi.org/10.1029/2006pa001278

Yamamoto, M., Oba, T., Shimamune, J., & Ueshima, T. (2004). Orbital-scale anti-phase variation of sea surface temperature in mid-latitude North Pacific margins during the last 145,000 years. *Geophysical Research Letters, 31*(16). https://doi.org/10.1029/2004gl020138

Yamamoto, M., Suemune, R., & Oba, T. (2005). Equatorward shift of the subarctic boundary in the northwestern Pacific during the last deglaciation. *Geophysical Research Letters, 32*(5), L05609. https://doi.org/10.1029/2004GL021903

Yamamoto, M., Yamamuro, M., & Tanaka, Y. (2007). The California current system during the last 136,000 years: response of the North Pacific High to precessional forcing. *Quaternary Science Reviews, 26*(3), 405–414. https://doi.org/10.1016/j.quascirev.2006.07.014

Zhang, S., Li, T., Chang, F., Yu, Z., Xiong, Z., & Wang, H. (2017). Correspondence between the ENSO-like state and glacial-interglacial condition during the past 360 kyr. *Chinese Journal of Oceanology and Limnology, 35*(5), 1018–1031. https://doi.org/10.1007/s00343-017-6082-9

Zhang, S., Yu, Z., Gong, X., Wang, Y., Chang, F., Lohmann, G., . . . Li, T. (2021). Precession cycles of the El Niño/Southern oscillation-like system controlled by Pacific upper-ocean stratification. *Communications Earth & Environment, 2*(239). https://doi.org/10.1038/s43247-021-00305-5

Zhao, M., Huang, C.-Y., Wang, C.-C., & Wei, G. (2006). A millennial-scale U37K′ sea-surface temperature record from the South China Sea (8°N) over the last 150 kyr: Monsoon and sea-level influence. *Palaeogeography, Palaeoclimatology, Palaeoecology, 236*(1-2), 39–55. https://doi.org/10.1016/j.palaeo.2005.11.033

Zuraida, R., Holbourn, A., Nürnberg, D., Kuhnt, W., Dürkop, A., & Erichsen, A. (2009). Evidence for Indonesian Throughflow slowdown during Heinrich events 3-5. *Paleoceanography, 24*(2). https://doi.org/10.1029/2008pa001653